Quantifying Pelvic Rotation on Digitally Reconstructed Radiographs

Wilco van de Velde

Erasmus MC

TU Delft Delft University of Technology

This page is intentionally left blank

Quantifying Pelvic Rotation on Digitally Reconstructed Radiographs

Wilco (W.J.C.) van de Velde
Student number: 4695437
30 mar 2026

Thesis in partial fulfilment of the requirements for the joint degree of Master of Science in

Technical Medicine

Leiden University ; Delft University of Technology ; Erasmus University Rotterdam

Master thesis project (TM30004 ; 35 ECTS)

Dept. of Orthopaedics and Sports Medicine, Erasmus MC

22 sep 2025 – 14 apr 2026

Supervisor(s):

Dr. Fleur Boel

Dr. Rintje Agricola

Thesis committee members:

Dr. ir. Bart Kaptein, LUMC (chair)

Dr. Fleur Boel, Erasmus MC

Dr. Rintje Agricola, Erasmus MC

This page is intentionally left blank

Preface

This thesis marks the end of my Master's program in Technical Medicine, and with that, of a rather lengthy period of studying at Delft University of Technology. It's been a peculiar journey: when I started with the Bachelor's program in Applied Physics, I didn't envision ending up with a Technical Medicine Master's degree. But here we are, and I feel privileged to have had the opportunity of studying at the crossroads of technology and medicine. To everyone who has been a part of this journey, I am very grateful.

I want to direct a special word of gratitude to the supervisors of my graduation internship, which culminated in the thesis you are now reading. Fleur, thank you for the tremendous amount of time and effort you have invested in me and this project. When I started this internship, given what had transpired before, I doubted (probably more than I realized at the time) whether I would ever finish this degree. Therefore, I am beyond grateful for the opportunity you and Rintje gave me at the Department of Orthopaedics & Sports Medicine. Your supervision, guidance and support have been vital to this project. Rintje, thank you for your supervision and critical eye throughout this project. Dr. Kaptein, thank you for taking the time to be a part of my thesis assessment committee. And finally, Mariëlle and Adriaan: thank you for your support during this final year.

Most of all, I am thankful to my family, who have been behind me every step of the way. We haven't had the easiest past few years, but knowing that you always had my back means more than words can express. And to my friends and roommates over the years: thank you for supporting and encouraging me, and thank you for the many invaluable memories we've made. I couldn't have done any of this without any of you.

As I close this part of my life and prepare to apply everything I've studied to the real world, I am excited to see what the future holds. Soli Deo Gloria.

Wilco van de Velde
Rotterdam, March 2026

Summary

Hip osteoarthritis is an important cause of disability and pain in adults, for which hip morphology is a significant risk factor. Hip morphology can be quantified using morphology measurements on pelvic radiographs. However, deviations in patient positioning, such as pelvic rotation, can influence the accuracy of these measurements. As a first step towards correcting pelvic rotation, this research proposes a model that quantifies pelvic rotation on digitally reconstructed radiographs (DRRs) using the area ratio of the obturator foramina.

Segmentations of the pelvis and both femurs of 30 randomly selected participants of the Generation R study were included. The segmentations had been created based on Magnetic Resonance Imaging scans. For each segmentation, DRRs were created with pelvic rotations ranging from -10° to +10° at 1° intervals. Landmarks were used to approximate the areas of the obturator foramina. The right-to-left ratio of the obturator foramen areas was calculated for each radiograph. To find the relationship between this ratio and the angle of pelvic rotation, one function was fitted to all results, and another to only the results for small angles (within ±5°). Both functions were inverted to predict the angle of rotation for a given obturator foramen area ratio. The resulting all-angle and small-angle models were validated on 30 DRRs with weighted random pelvic rotation taken from 15 different participants of the Generation R study, with a 3:1 split between small and large (between ±6° and ±10°) angles of rotation.

An exponential function was found to best describe the relationship between the obturator foramen area ratio and the angle of pelvic rotation. The all-angle model had a median deviation of -0.5° [IQR: -2°, 1°] from the true angles of rotation, and estimated the angle of rotation within 2° in 73% of cases. The small-angle model had a median deviation of 0° [IQR: -2°, 2°] and was accurate within 2° in 67% of cases. When assessing accuracy only for small angles of rotation, the median deviations were -1° [IQR: -2°, 1°] and -0.5° [IQR: -2°, 1°], and the accuracy percentages were 86% and 73%, respectively.

The proposed models showed moderate performance in assessing pelvic rotation. The results of both models are quite similar, though the all-angle model was more significantly influenced by increased variance at larger angles of rotation. While further improvement of the models is necessary, these performances show that quantification of pelvic rotation based on the obturator foramen area ratio on radiographs is possible. As such, this research is a promising first step towards correcting pelvic rotation and improving hip morphology measurements.

Table of Contents

Introduction

Osteoarthritis (OA) is a major cause of pain and disability worldwide [1]. It is estimated that around one in seven people will develop some form of OA during their lifetime. The hip is the third most commonly affected joint after the knee and hand [2]. Multiple risk factors have been identified for the development of hip OA, including age, body mass index, genetics and occupation [3]. It has also been shown that deviations in hip morphology significantly contribute to the development of hip OA [4-6].

Assessment of hip morphology is commonly done through pelvic radiographs, though Dual Energy X-Ray Absorptiometry (DXA) scans have been shown to be a good alternative [7]. Quantitative measurements of various angles and distances within the hip joint are used to describe hip morphology on these scans. Traditionally, such measurements are performed manually, but an automated method has been described in recent literature [8]. Conventional measurements have an important downside: they reduce the rather complex hip shape to a single or a few values. This limits the amount of information that such measurements can convey, essentially leading to an oversimplification of the hip shape. To combat this problem, Statistical Shape Modelling (SSM) can be used as an alternative method. SSM gives a mathematical description of the mean hip shape and the main modes of variation across a population [9, 10]. It describes an individual's deviation in hip shape from the mean hip shape of the population, by quantifying the relative impact of various shape variations. This allows for specific analysis of these variations and their relationships to diseases such as OA. SSM has been shown to include information that was absent from traditional morphology measurements [11]. At present, SSMs of the hip are primarily used for research purposes, but clinical applications exist as well [12].

Both traditional hip morphology measurements and SSM are subject to an important limitation when applied to two-dimensional imaging: results can be affected by patient positioning. Even when standardized imaging protocols are followed, deviations in patient positioning, such as pelvic tilt, pelvic rotation and femoral rotation, can occur. Multiple authors have shown that such inaccuracies can introduce significant deviations into traditional measurement results [13-16]. Recent research found that femoral rotation influences SSM results, primarily affecting the first few shape modes [17].

Due to the two-dimensional nature of pelvic radiographs and DXA scans, it is difficult to accurately distinguish between real anatomic shape variations and positioning-induced deviations. This introduces a margin of error in the results of morphology measurements and SSM. Therefore, it is crucial to correct the influence of patient positioning on these scans. Several authors have attempted to quantify pelvic tilt and femoral rotation on radiographs [18-20]. For pelvic rotation, Kanazawa et al. proposed an equation that uses the sizes of the obturator foramina to estimate rotation [21]. However, to the best of my knowledge, no method currently exists for the correction of these deviations. This research attempts to fill that knowledge gap by proposing a novel, viable method to quantify and correct pelvic rotation on radiographic images.

The aim of this thesis is to develop a quantification model for pelvic rotation, using the relative sizes of the obturator foramina. These are determined based on two-dimensional projections of bone segmentations of the pelvis, which were created using Magnetic Resonance Imaging (MRI) data. The performance of the model will be validated on projections with known rotation from unused bone segmentations.

Methods

Participant inclusion

MRI scans of participants of the Generation R Study were used for this research. This population-based cohort study examined children at regular intervals from fetal life until adulthood. Its design has been described in detail elsewhere [22, 23]. During the Generation R study, MRI scans were obtained at multiple time points. Thirty scans of participants aged around 18 years were randomly selected for the development of the quantification method for pelvic rotation. A separate dataset was created for validation of the proposed method, consisting of 15 randomly selected participants not included in the initial dataset.

Bone segmentations

Bone segmentations of the pelvis and both femurs were extracted from the MRI scans. Computed Tomography (CT) is more commonly used to examine bony structures, but it exposes subjects to ionizing radiation, which carries an increased risk of cancer [24]. For this reason, since participants are young and healthy, MRI scans were preferred in the Generation R study. Literature shows that MRI data can be used to create accurate bone models [25, 26]. Kamphuis et al. have described the use of a neural network (nnU-Net) to create MRI-based segmentations of the hip [27]. On the Generation R dataset, their model reached a Dice score of 0.90±0.01 for acetabular bone segmentation [28]. The segmentations used for this thesis had already been created for other research. An example slice from a bone segmentation is shown in Figure 1a.

The segmentations did not include density information, since they were binary and based on MRI data. To address this problem, the difference between cortical and trabecular bone was simulated. To simulate cortical bone, the segmentation was shrunk along all edges and the difference between the original segmentation and the shrunken one was labeled as cortical bone. Cortical bone is estimated to have three times the density of trabecular bone [29]. Therefore, the simulated cortical layer was given a pixel value that was three times as high as the pixel value of the original segmentation. Since the pelvis had a total thickness of only about 5 to 10 pixels in most segmentations, the pelvic cortical bone was given a thickness of one pixel. The femur had a cortical thickness of two pixels, corresponding to around 10% of the total bone thickness. Figure 1b shows a slice of the bone segmentation after simulating cortical and trabecular bone.

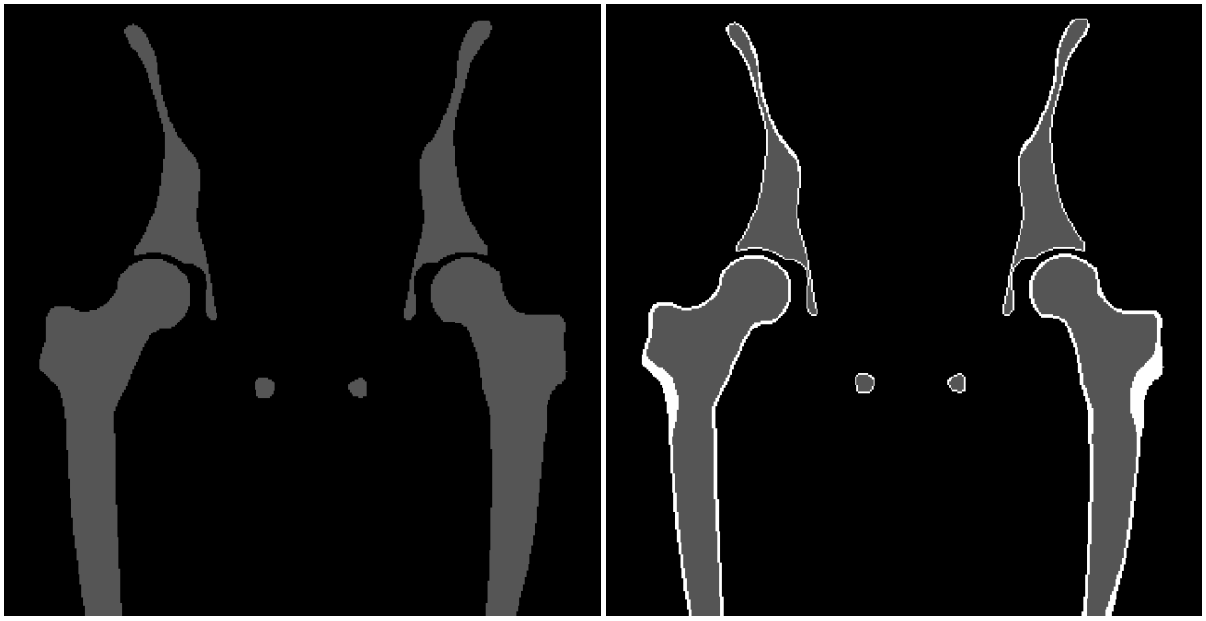

(a) (b)

Figure 1. Example of the bone segmentation used in this research. (a) Coronal slice of the original bone segmentation of the pelvis and femurs. (b) Coronal slice of the bone segmentation after adding simulated cortical bone. The femur has a cortical thickness of two pixels. The pelvis has a cortical thickness of one pixel.

Digitally Reconstructed Radiographs

Digitally Reconstructed Radiographs (DRRs) were created from the segmentations using the DiffDRR pipeline [30]. DRRs are simulated X-ray images taken from three-dimensional (3D) data, taken from various angles to simulate pelvic rotation. For each participant, anteroposterior DRRs were created with rotations ranging from -10 degrees to +10 degrees, with an interval of one degree between each radiograph. Negative rotation was defined as anterior rotation of the right hip and posterior rotation of the left hip. The axis of rotation was placed in the pubic symphysis. An example DRR at neutral rotation is given in Figure 2a.

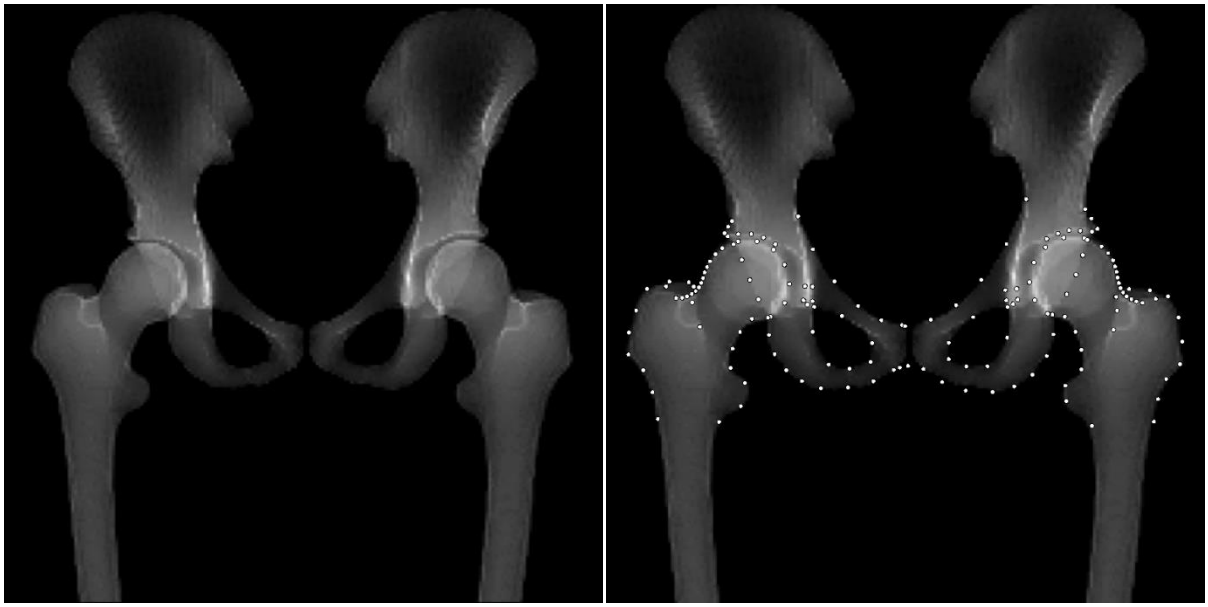

(a) (b)

Figure 2. (a) A digitally reconstructed radiograph (DRR) created from a bone segmentation, created at neutral rotation. (b) Landmarks on the DRR shown in subfigure (a).

Obturator foramen analysis

The DRRs were subsequently analyzed using BoneFinder [31]. This software automatically identifies 80 landmarks on each hip joint (160 when analyzing both hips in the same image), giving each landmark a specific number. Seven landmarks are placed along the edges of each obturator foramen. The protocol for the placement of these landmarks can be found in Appendix A. After the automatic analysis, the landmark placements of the obturator foramina were manually corrected as needed. An example of the landmark placement after manual correction can be seen in Figure 2b. To account for the rounded shape of the obturator foramen, a periodic spline was created based on the corrected landmarks. This is a mathematical function fitted to the points of the obturator foramen, describing a smooth curve approximating its shape. As shown in Figure 3, a spline gives a more accurate representation of the obturator foramen area than connecting each point with a straight line. The area of this spline was calculated and used as an estimate of the area of the obturator foramen. For each DRR, the ratio between the areas of the right and left obturator foramen was calculated.

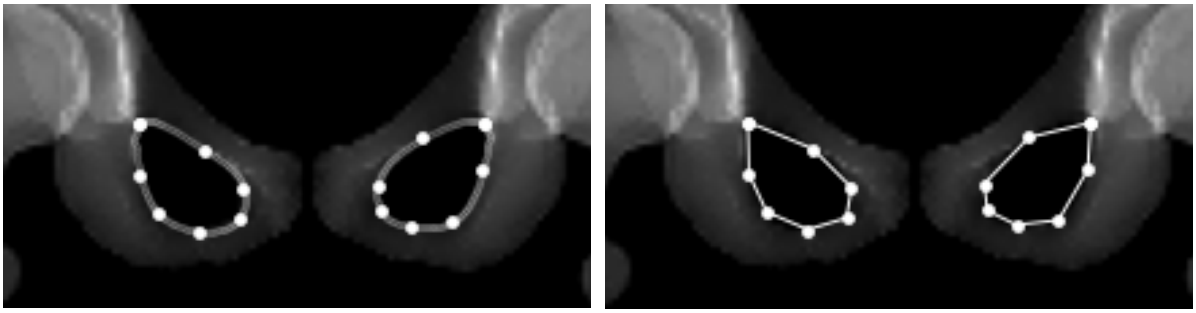

(a) (b)

Figure 3. Comparison of a spline (figure a) and a straight line (figure b) approximation of the obturator foramen area. The spline approximation follows the rounded contour of the obturator foramen more accurately.

Relationship between ratio and rotation

All obturator foramen area ratios were determined, and the median and IQR were calculated for each angle of pelvic rotation. Basic linear, quadratic and exponential functions were fitted to the median, to find the general relationship between the angle of rotation and the obturator foramen area ratio. The accuracy of these models was compared using the Akaike Information Criterion (AIC). This is a statistical measure for the relative accuracy of a model when describing a dataset. It is calculated by the equation

$$AIC = -2\ln\hat{L} + 2k, \tag{1}$$

in which $\hat{L}$ indicates the maximized likelihood, and k is the number of model parameters that needs to be estimated [32]. Since the errors in this research are distributed normally, this can be rewritten as

$$AIC = 2k + n\ln\frac{RSS}{n}, \tag{2}$$

in which n is the number of data points, RSS is the Residual Sum of Squares of the data, and k again is the number of estimated parameters.

The model with the lowest AIC was taken to be the most accurate. This model was then further refined by fitting it to the full dataset, yielding a function that described the obturator foramen area ratio as a function of the angle of rotation. Finally, this resulting function was inverted, leading to a model that estimates the angle of rotation based on the obturator foramen area ratio. For extreme angles of rotation, one obturator foramen becomes very small and the other becomes very large, leading to exponential changes in the obturator foramen area ratio. As a result, the variance of the

area ratio for large angles of rotation was expected to be very high, influencing the fitting process and thereby reducing the overall accuracy of the model. Furthermore, angles of rotation between -5° and 5° were taken to be more clinically relevant, since larger angles of rotation are unlikely to occur when protocols are followed adequately. Therefore, a secondary analysis was carried out that specifically investigated these smaller angles of rotation. To this end, a second model was created by following these same steps, but only using pelvic rotations between -5° and 5° to find the best fitting function. This secondary model was called the 'small-angle model'. The original model including all angles was dubbed the 'all-angle model'.
The results of both models were also compared to a proposed formula by Kanazawa et al. that uses the height and width ratios of the obturator foramina to estimate pelvic rotation [21]:

$$Rotation\ (male{:}\ female) = (19.9{:}\,24.2) + (2.1{:}\,3.6) * \frac{H_{right}}{W_{right}} + (0.9{:}\,1.5) \times \frac{H_{left}}{W_{left}} - (23.2{:}\,25.1) * WR. \quad (3)$$

In this equation, *H* indicates the height of the obturator foramen, defined as the difference in the y-direction between the highest and lowest point of the obturator foramen. *W* indicates the width of the obturator foramen, defined as the difference in the x-direction between the most medial and the most lateral point of the obturator foramen. *WR* is the width ratio between the right and left obturator foramen (W_{right}/W_{left}). In our research, the height and width measurements are based on the spline approximation of the obturator foramen, as visualized in Figure 4. The coefficients are gender-specific: for each part of the equation, the first coefficient is used for male subjects and the second for female subjects.

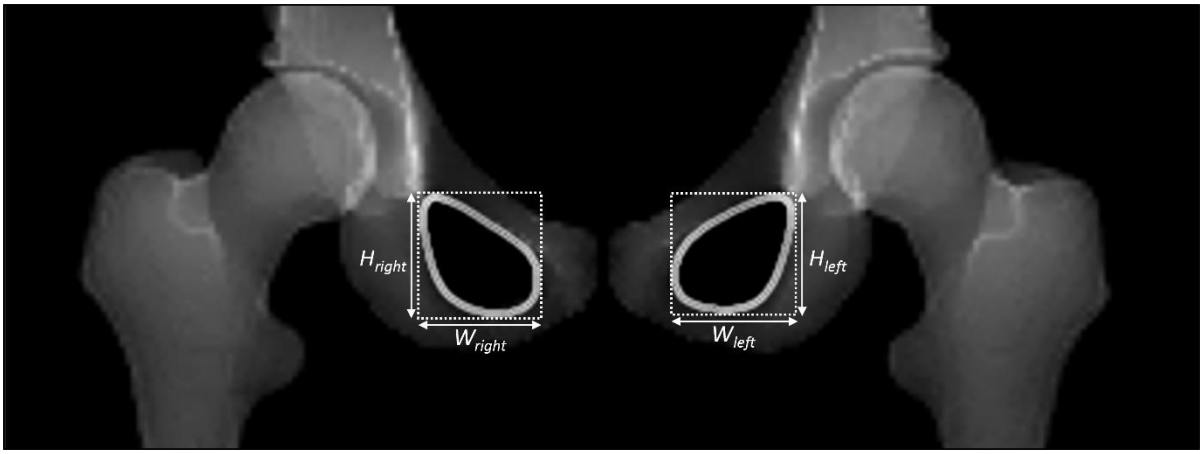

*Figure 4. Visualization of the height (H) and width (W) measurements of the obturator foramina based on the spline approximation, as used in Equation (*3*. H is the distance in the y-direction between the highest and lowest point of the spline. W is the distance in the x-direction between the most medial and the most lateral point of the obturator foramen.*

Validation

The models found in the previous steps were validated using 15 additional participants, who were not in the initial dataset. For each of these participants' MRI scans, two DRRs were created with known, random rotations, resulting in a total of 30 DRRs. The randomization of these rotations was weighted, with a 3:1 split between small (±5° or smaller) and large (between ±6° and ±10°) angles. The obturator foramen ratios were determined, and both models as well as the formula by Kanazawa et al. (Equation (*3*)) were separately applied to the data to obtain an estimate of the pelvic rotation. The results of all three models were visually analyzed using scatter plots. The results of both proposed models were also compared using Bland-Altman analyses.

Software

Image processing and data processing were performed using Python, version 3.12 [33]. DRRs were created with DiffDRR version 0.6.0. BoneFinder version 1.3.0 was used for the landmark placement. The periodic spline for the obturator foramen approximation and the exponential model were fitted with SciPy 1.17.0 [34].

Results

Participant inclusion

Thirty participants were randomly selected from the Generation R dataset and included in the training set. An additional fifteen different random participants were included in the validation set. The median age of the participants included in the training set was 18.9 years. Participants included in the validation set had a median age of 19.5 years. In the training set, 43% of participants were male and 10% had a non-Western background. The validation set consisted of 47% males and had 26% non-Western participants. A more detailed overview of the characteristics of the included participants is presented in Table 1.

Table 1. General characteristics of the included participants in both datasets.

	Training set (n=30)	**Validation set (n=15)**
Age (years)	18.9 [18.7, 19.4]	19.5 [19.1, 19.9]
Gender		
Male	13 (43)	7 (47)
Female	17 (57)	8 (53)
Ethnicity		
Western	27 (90)	11 (73)
African	0 (0)	2 (13)
Asian	1 (3)	2 (13)
Other non-Western	2 (7)	0 (0)

Continuous variables are presented as median [IQR]. Discrete variables are presented as n (%)

Image processing

Twenty-one DRRs were constructed for each participant, representing angles of pelvic rotation between -10° and +10° with 1° intervals. This yielded a total of 630 DRRs in the training set. A subset of the created DRRs for one participant is presented in Figure 5. The landmarks were automatically placed on all DRRs, and manual point corrections were performed when necessary. Figure 6 shows the obturator foramen landmarks with splines describing the outline of the obturator foramen for the DRRs. The obturator foramen area ratios were determined for each DRR. These are visualized in Figure 7, as well as the median value and IQR for each angle of rotation.

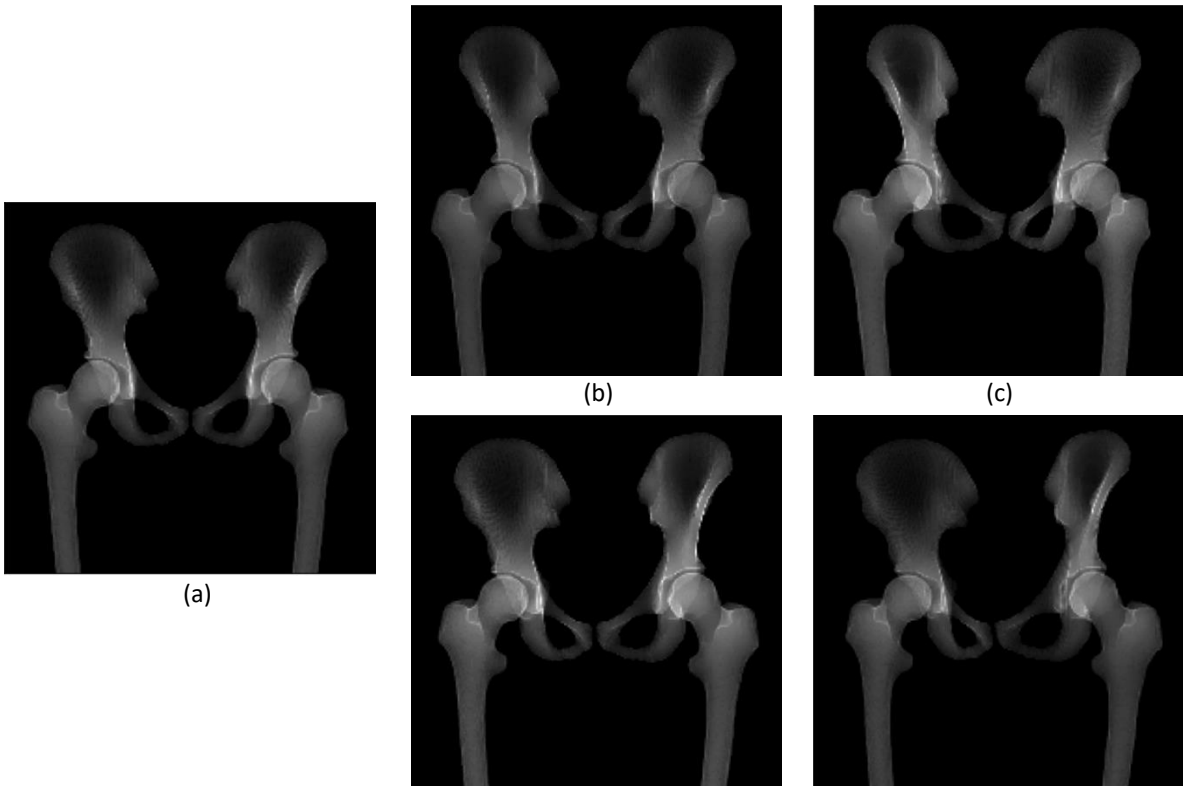

Figure 5. Rotated Digitally Reconstructed Radiographs (DRRs) of one participant. (a) DRR in neutral position (0° rotation). (b) DRR with -5° rotation. (c) DRR with -10° rotation. (d) DRR with +5° rotation. (e) DRR with +10° rotation.

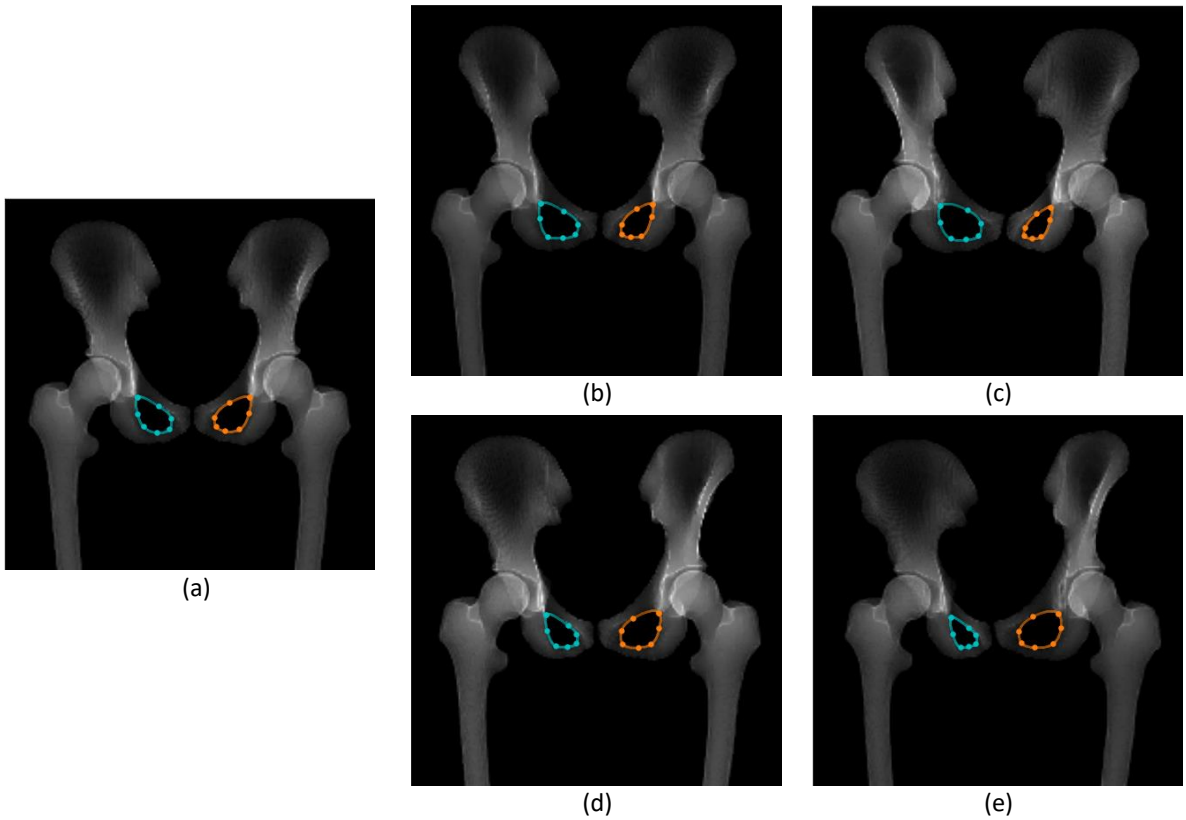

Figure 6. DRRs of the same participant as in Figure 5. The obturator foramen landmarks are indicated in blue (right) and orange (left), as well as the spline approximation. (a) DRR in neutral position (0° rotation). (b) DRR with -5° rotation. (c) DRR with -10° rotation. (d) DRR with +5° rotation. (e) DRR with +10° rotation.

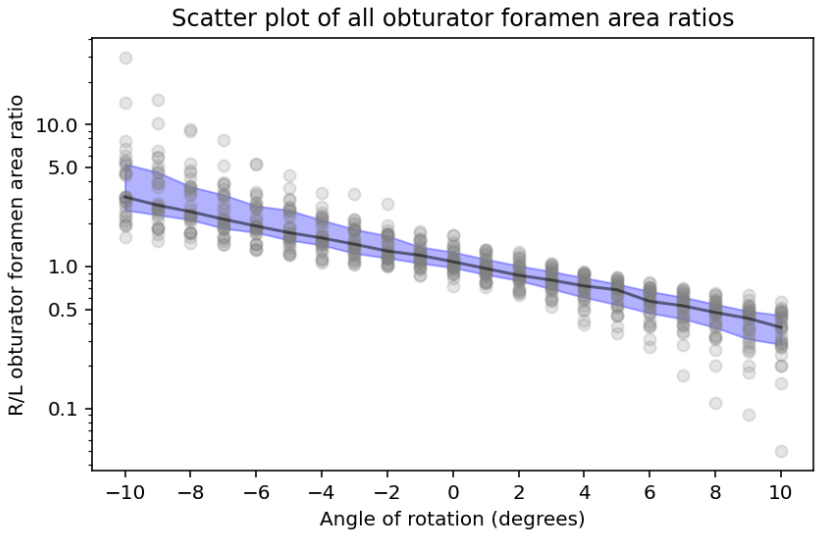

Figure 7. Scatter plot showing the measured R/L obturator foramen area ratio for each angle of rotation. The red line indicates the median measurement for each angle. The shaded blue area represents the interquartile range. The y-axis is logarithmic.

Relationship between ratio and rotation

To identify the model that best described the relationship between the obturator foramen area ratio and the angle of pelvic rotation, the AIC was calculated for basic linear, quadratic and exponential fits to the median obturator foramen area ratio. The results are presented in Table 2. The exponential fit had the lowest AIC value and was used as the basis for the best-fit function.

Table 2. Akaike Information Criterion (AIC) values for each of the basic models.

Model	**AIC value**
Linear	-59.68
Quadratic	-108.65
Exponential	-139.06

The exponential model had the following shape:

$$R/L = a * e^{b * rot} + c. \quad (4)$$

In this equation, *R/L* indicates the R/L ratio of the obturator foramen areas ($Area_R/Area_L$), *rot* is the angle of rotation in degrees, and *a*, *b* and *c* are the parameters to be optimized. The coefficients of the exponential fit used for the AIC calculation were taken as the starting values for the optimization. These values were *a* = 1.0, *b* = -0.1 and *c* = 0.0. When fitting this model to the full dataset including all angles of rotation, the best-fit function was

$$R/L = 0.64 * e^{-0.19 * rot} + 0.38. \quad (5)$$

When fitted only to the smaller angles (within ±5°), the best-fit function was

$$R/L = 0.94 * e^{-0.13 * rot} + 0.17. \quad (6)$$

The estimated area ratios for both models are plotted in Figure 8, together with the median and IQR of the measured area ratios for each angle.

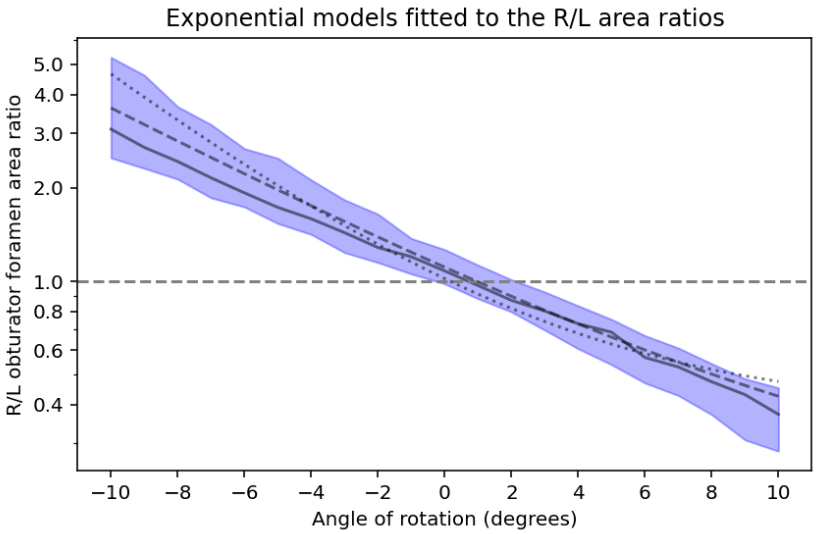

Figure 8. Plot showing the exponential functions fitted to the data. The solid red line is the median of the measured R/L area ratios for each angle. The shaded blue area indicates the interquartile range (IQR) of the measurements. The dotted line represents the function fitted to the data for all angles. The dashed line represents the function fitted to the data corresponding to the smaller angles (within ±5°). The y-axis is logarithmic.

Both models were rewritten to estimate the angle of pelvic rotation for known obturator foramen area ratios. The resulting all-angle model gives the following relationship:

$$Rot = -5.3\ln(1.6 * R/L - 0.6). \quad (7)$$

The small-angle model describes the relationship as:

$$Rot = -7.7\ln(1.1 * R/L - 0.2). \quad (8)$$

Validation

To validate the accuracy of the model, a separate dataset consisting of 15 participants was created. For each participant, two DRRs with random, integer rotation were created. A 3:1 split between small and large angles of rotation was ensured. In Figure 9, a histogram of all angles of rotation in the validation set is presented.

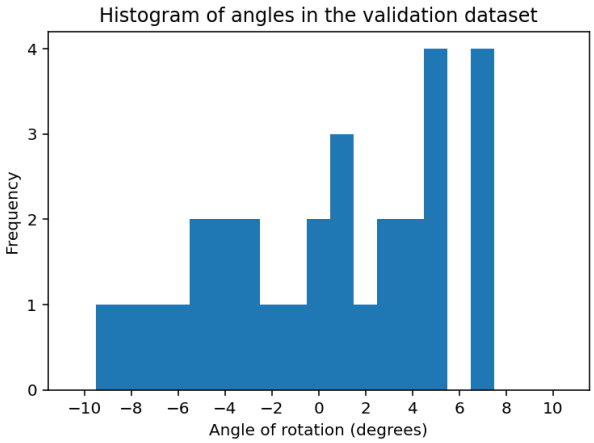

Figure 9. Histogram of the angles of rotation included in the validation dataset.

For each DRR, the obturator foramen area ratio was measured. This ratio was used as input in Equations (*7* and (*8* to estimate the amount of pelvic rotation for each DRR. The results for both

models are visualized in Figure 10. Figure 10a shows the results for the all-angle model (Equation (*7*), and Figure 10b shows the results for the small-angle model (Equation (*8*). A Bland-Altman plot directly comparing the results of both models is shown in Figure 11. The same DRRs were also analyzed with the Kanazawa model (Equation (*3*)). The results are visualized in Figure 12.

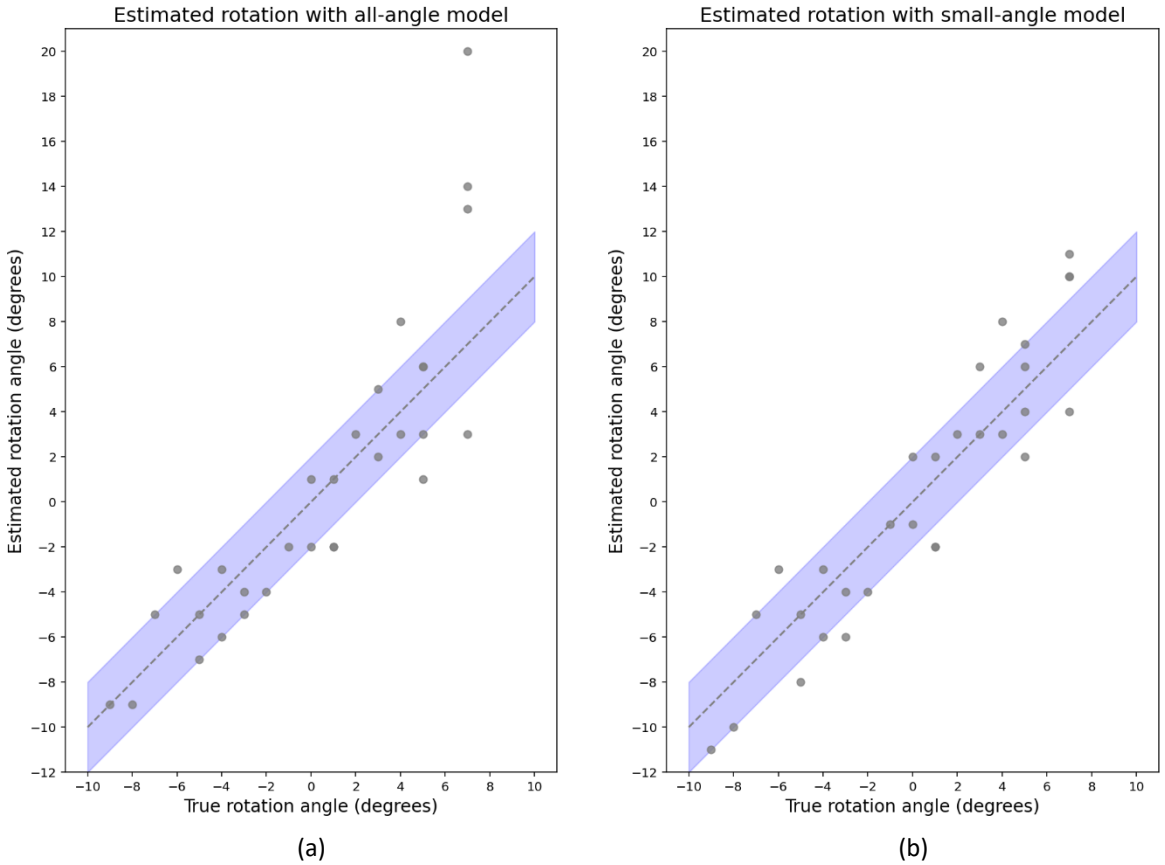

Figure 10. Comparison of the results of the all-angle model (a) and the small-angle model (b). The dots represent the estimations. The dotted line is the correct estimation for each angle. The shaded area shows a range of ±2° around the correct estimation.

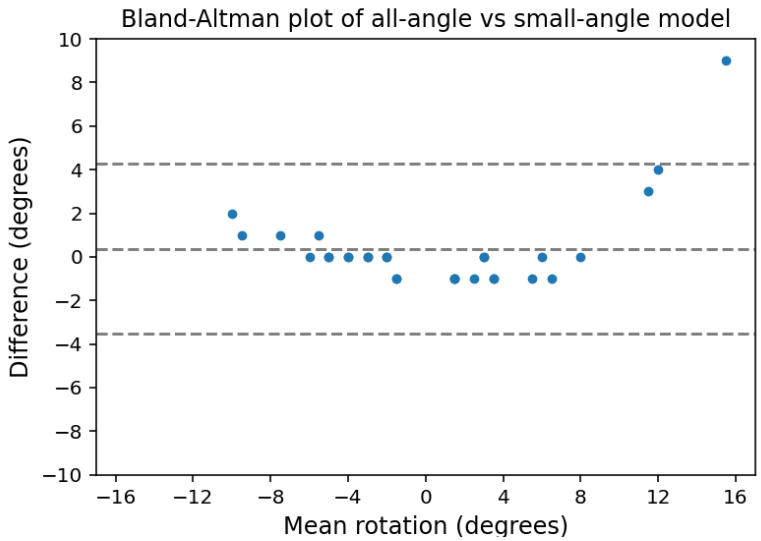

*Figure 11. Bland-Altman plot comparing the all-angle model to the small-angle model. On average, the all-angle model estimate is 0.4° higher than the small-angle model estimate. The limits of agreement, defined as mean ± 1.96*SD, are -3.5° and 4.3°. SD = standard deviation.*

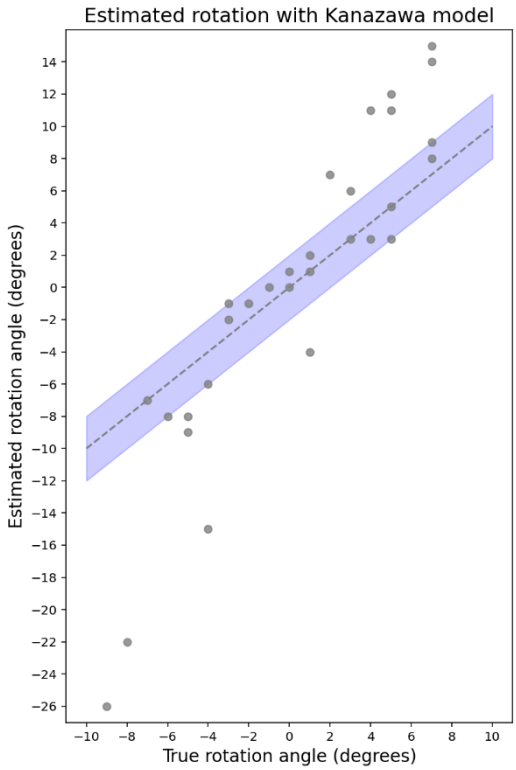

Figure 12. Results of the Kanazawa model. The dots represent the estimations. The dotted line is the correct estimation for each angle. The shaded area shows a range of ±2° around the correct estimation.

The accuracy of each model was assessed for all angles and for only the small angles. The results are displayed in Table 3.

Table 3. Accuracy metrics of the results of the models

	All angles (±10°)		**Small angles (±5°)**	
	Deviation (°)	**Accuracy (%)**	**Deviation (°)**	**Accuracy (%)**
All-angle model	-0.5 [-2, 1]	73	-1 [-2, 1]	86
Small-angle model	0 [-2, 2]	67	-0.5 [-2, 1]	73
Kanazawa model	0.5 [-2, 2]	57	0.5 [-2, 2]	59

The accuracy metrics are given for all angles and for only angles within ±5°. The 'Difference' columns show the median deviation of the results of the models and the true angles of pelvic rotation, as well as the interquartile range of these deviations. Since the validation set included an even number of samples, the median was defined as the arithmetic mean of the two middle values. The 'Accuracy' columns show the percentage of estimates for which the difference is 2° or less.

Discussion

This research proposes a quantification method for pelvic rotation on radiographs using the ratio of the obturator foramen areas. An exponential correlation was found between this ratio and pelvic rotation. The accuracy of the proposed models was moderate: the model trained on all angles of rotation reached an accuracy of 73%, and the model trained only on smaller angles of rotation achieved 67%. These results are promising and indicate that this method has the potential to be of value in clinical and research practice.

The results of this research give rise to a number of observations. First of all, the overall performance of both models is moderate: roughly two-thirds of the data points are estimated with an accuracy of ±2°, and the median difference between the estimated and true rotations is close to zero.
Secondly, the all-angle model exhibits several large outliers at higher angles of rotation. This is a logical result of the fact that the area ratio changes exponentially when the angle of rotation increases, since the observed area of one obturator foramen increases while the other decreases. Therefore, the variance increases for larger angles. Since the training set included significant variance in the higher rotations, it makes sense that the model accuracy decreased significantly at large angles of rotation. When only training on the small angles, the influence of this higher variance is negated, resulting in a much smaller deviation even for large angles of rotation. This is also reflected in the increased accuracy of both models when only assessing smaller angles.
Thirdly, the results of both models are quite similar. Surprisingly, the all-angle model has a slightly higher accuracy percentage than the small-angle model, even at the smaller angles of rotation. Since the small-angle model was specifically trained on small angles, it would be expected to perform better on this subset. However, this difference is caused by very small variations between individual points: multiple estimates that are right on the ±2° edge for the all-angle model fall just outside of that limit for the small-angle model, indicating that the results of both models are indeed very similar. A possible cause of the differences between the results of the models is that the all-angle model tends to give a slightly lower estimate than the small-angle model at smaller angles. This is a consequence of the fact that the area ratios for large angles of rotation influence the fitting process of the all-angle model. As noted before, some outliers are present at these extreme rotations, causing the fit to be skewed towards higher values for these angles. This leads to a slightly lower fit for smaller angles. All in all, the results of both models are very close, and neither model significantly outperforms the other.

To the best of my knowledge, the proposed method is novel, and no literature exists that describes the use of obturator foramen area ratios to estimate pelvic rotation. The closest related work is by Kanazawa et al., who used manual measurements of the height and width ratios of the obturator foramina to estimate pelvic rotation [21]. Their model (Equation (*3*)) was developed on CT-based DRRs with only positive rotations between 0° and +20°, in 5° intervals. The authors also incorporated different degrees of pelvic tilt. Their results showed a gender-related difference in obturator foramen width and height ratios, leading to different coefficients for male and female subjects. When applying their model to our data (see Figure 12), the results are quite inaccurate: only 57% of the estimates fall within ±2° of the true rotation. Especially at higher angles of rotation, the deviations are very large. At smaller angles, the accuracy does not significantly increase, although the individual deviations are less extreme. For angles within ±5°, 59% of estimates are accurate within 2 degrees. A number of possible reasons can explain this observation. This model was only developed on rotations in the positive direction, whereas our data also includes rotations in the negative direction. This likely results in the extreme inaccuracies seen for larger negative angles of rotation. At positive angles of rotation, while still significant, the deviations are smaller. Furthermore, 5° rotation intervals were used, as opposed to the 1° intervals used in our research. Finally, as Kanazawa et al. note, their sample of 10 participants was rather small and homogeneous. These factors limit the generalizability of their model, as shown by its poor performance in the current study.

The most important limitation of this research is the lack of standardization of patient positioning, including pelvic rotation, of the MRI scans prior to the creation of the bone segmentations. For the introduction of pelvic rotation and the creation of DRRs, the orientation of the MRI scans was taken as the 'neutral' position (0° rotation). If any pelvic rotation was present on these MRI scans, it would have carried over into the results and influenced the models. Additionally, no secondary analysis was conducted to investigate differences between genders, even though gender-related differences in the obturator foramen shape exist. However, while the height-width ratio of males and females is indeed different, we assumed that these shape differences are largely symmetrical and therefore would not impact the area ratio. Another limitation of this research is the use of a sample of only 30 participants. This means that individual participants have a relatively big influence on the model. Therefore, if a participant has an unusual obturator foramen shape, this could significantly impact the model and limit its generalizability. The high number of DRRs created for each participant somewhat negates this limitation, since the total of 630 datapoints is high, but the datapoints are not independent. Therefore, this likely limits the accuracy of our model when applied to data outside of the training set. Finally, the obturator foramen area was estimated from seven landmarks, rather than a full segmentation of the obturator foramen. The area of the obturator foramen was estimated based on a spline through these landmarks, which may have introduced inaccuracies in the estimate of the area and the subsequent area ratio calculation. However, improvement of the area segmentation is expected to only result in small changes of the total area, and thus the impact on the ratio is expected to be minimal.

This research also has several strengths. First, the data were taken from the Generation R dataset, an open population, prospective cohort in the region of Rotterdam, the Netherlands. This is a very diverse cohort with participants from many different ethnic backgrounds. Since the proposed models were trained and validated on a diverse group of participants, their generalizability is higher. Therefore, it is likely that these models will yield similar results across different population groups. Second, the use of DRRs at rotation intervals of only one degree allowed for a detailed analysis of the correlation between the obturator foramen area ratio and pelvic rotation. Third, the simulation of cortical bone ensured that the DRRs very closely resembled real radiographs, even though the segmentations were based on MRI data. Therefore, we expect the proposed method to be generalizable to radiographs.

Since both models have shown similar potential, it is difficult to choose which model to focus on for further development. The small-angle model has the advantage of being less susceptible to outliers, and small angles are more clinically relevant. Hence, it is likely that this model will eventually be more applicable to clinical practice than the all-angle model. However, it may be worthwhile to first improve the training dataset for both models and observe how their performances develop before definitively shifting the focus to one model. The most important factor in improving the training dataset is increasing the number of independent data points. This can of course be achieved by including more participants in the dataset. We recommend considering to not include DRRs at all angles of rotation for each participant, but rather using a small number of DRRs at random angles of rotation. In contrast to the 21 DRRs per patient used in this research, such an approach would limit the influence of individual participants. Besides, it would allow for weighting the distribution of the angles of rotation as desired. A similar approach was used for the validation set in this research, the size of which should also be increased to allow for more definitive conclusions about the model performance. It is recommended to continue using the Generation R dataset when adding participants, as its size and diversity make it well suited to this research.
Another avenue to improve this research is to investigate the margins of error of these models. In this research, only the accuracy and median deviation from the true angles have been analyzed. While this provides a reasonable indication of the model performance, it does not quantify the

reliability of individual predictions. Quantifying the margins of error of the models would help better understand the their performance and is therefore an important step towards their application in practice. Furthermore, if these models are used as a basis for a correction method for pelvic rotation, their margins of error are crucial for determining the reliability of the corrections.
Further research can also focus on developing a fully automatic method to determine the obturator foramen area. As noted before, the landmarks needed manual corrections to ensure a proper approximation of the obturator foramen. This is time-consuming and introduces potential inter- or intra-rater variability, which could influence the accuracy of the approximation. Automating this process would combat both of these issues, leading to faster and more consistent calculations of the obturator foramen area ratio.
Finally, once these models have been sufficiently improved to allow for proper quantification of pelvic rotation, the next step is to develop a correction method for pelvic rotation in the context of hip morphology measurements. Multiple approaches exist, such as correcting the morphology measurement results, adapting the methodology used for these measurements, or even correcting the images themselves to account for pelvic rotation. Further research is required to find the most viable and reliable correction method, depending on the context in which pelvic rotation is desired.

While the accuracy of the proposed models can be improved, the method used in this research shows clear potential in clinical and research practice. Radiographs offer substantial practical advantages over three-dimensional imaging modalities such as CT and MRI: they are much quicker, cheaper and easier to implement. For patients, radiographs are less taxing than 3D scans, and, compared to CT scans, carry a much lower radiation burden. Improving the accuracy of radiographic hip morphology measurements, for instance by adequately correcting pelvic rotation, would allow clinicians and researchers to depend on radiographs rather than CT or MRI scans for hip morphology assessments. This would positively impact both patient well-being and healthcare costs. The proposed method for quantifying pelvic rotation forms an important first step towards that goal.

In conclusion, a quantification method for pelvic rotation on hip radiographs was developed by correlating the obturator foramen area ratio with the angle of rotation. Although the models' accuracies can be further improved, the results are promising: pelvic rotation can be quantified from two-dimensional scans, representing an important first step towards its correction. Future research should focus on refining these models to improve quantification accuracy and on developing a correction method for hip morphology measurements.

Acknowledgements

The Generation R Study is conducted by the Erasmus MC, University Medical Center Rotterdam in close collaboration with the Erasmus University Rotterdam and the city of Rotterdam. We gratefully acknowledge the contribution of children and parents. The general design of Generation R Study is made possible by long-term financial support from Erasmus MC, University Medical Center Rotterdam, the Netherlands, Organization for Health Research and Development (ZonMw) and the Ministry of Health, Welfare and Sport

Data availability

The code used for this research is available upon request at the author or thesis supervisor. BoneFinder® is freely available from the website (www.bone-finder.com; The University of Manchester, UK) [31].

References

1. Hunter DJ, Bierma-Zeinstra S. Osteoarthritis. Lancet. 2019;393(10182):1745-59.
2. Zhang X, Huang C, Hu Z, Tan Y, Wang P, Zhu L, et al. Global, regional, and country-specific lifetime risks of osteoarthritis, 1990-2021: a systematic analysis for the global burden of disease study 2021. Glob Health Res Policy. 2025;10(1):29.
3. Murphy NJ, Eyles JP, Hunter DJ. Hip Osteoarthritis: Etiopathogenesis and Implications for Management. Adv Ther. 2016;33(11):1921-46.
4. Casartelli NC, Maffiuletti NA, Valenzuela PL, Grassi A, Ferrari E, van Buuren MMA, et al. Is hip morphology a risk factor for developing hip osteoarthritis? A systematic review with meta-analysis. Osteoarthritis Cartilage. 2021;29(9):1252-64.
5. Ganz R, Parvizi J, Beck M, Leunig M, Notzli H, Siebenrock KA. Femoroacetabular impingement: a cause for osteoarthritis of the hip. Clin Orthop Relat Res. 2003(417):112-20.
6. Riedstra NS, Boel F, van Buuren MMA, Ahedi H, Arbabi V, Arden N, et al. Acetabular dysplasia and the risk of developing hip osteoarthritis within 4-8 years: An individual participant data meta-analysis of 18,807 hips from the World COACH consortium. Osteoarthritis Cartilage. 2025;33(3):373-82.
7. Boel F, Wortel J, van Buuren MMA, Rivadeneira F, van Meurs JBJ, Runhaar J, et al. DXA images vs. pelvic radiographs: Reliability of hip morphology measurements. Osteoarthritis Cartilage. 2025;33(2):283-92.
8. Boel F, de Vos-Jakobs S, Riedstra NS, Lindner C, Runhaar J, Bierma-Zeinstra SMA, et al. Automated radiographic hip morphology measurements: An open-access method. Osteoarthr Imaging. 2024;4(2):100181.
9. Cootes TF, Taylor CJ, Cooper DH, Graham J. Active Shape Models-Their Training and Application. Computer Vision and Image Understanding. 1995;61(1):38-59.
10. Sarkalkan N, Weinans H, Zadpoor AA. Statistical shape and appearance models of bones. Bone. 2014;60:129-40.
11. Waarsing JH, Rozendaal RM, Verhaar JA, Bierma-Zeinstra SM, Weinans H. A statistical model of shape and density of the proximal femur in relation to radiological and clinical OA of the hip. Osteoarthritis Cartilage. 2010;18(6):787-94.
12. Johnson LG, Bortolussi-Courval S, Chehil A, Schaeffer EK, Pawliuk C, Wilson DR, et al. Application of statistical shape modeling to the human hip joint: a scoping review. JBI Evid Synth. 2023;21(3):533-83.
13. Henebry A, Gaskill T. The effect of pelvic tilt on radiographic markers of acetabular coverage. Am J Sports Med. 2013;41(11):2599-603.
14. Monazzam S, Agashe M, Hosalkar HS. Reliability of overcoverage parameters with varying morphologic pincer features: comparison of EOS(R) and radiography. Clin Orthop Relat Res. 2013;471(8):2578-85.
15. Monazzam S, Bomar JD, Agashe M, Hosalkar HS. Does femoral rotation influence anteroposterior alpha angle, lateral center-edge angle, and medial proximal femoral angle? A pilot study. Clin Orthop Relat Res. 2013;471(5):1639-45.
16. O'Connor JD, Rutherford M, Hill JC, Beverland DE, Dunne NJ, Lennon AB. Effect of combined flexion and external rotation on measurements of the proximal femur from anteroposterior pelvic radiographs. Orthop Traumatol Surg Res. 2018;104(4):449-54.
17. Donkervoort C. A Study of 3D Femoral Rotational Effects on X-ray Femoral Shapes Using Statistical Shape Modelling: Delft University of Technology; 2024.
18. Muir JM, Vincent J, Schipper J, Gobin VD, Govindarajan M, Fiaes K, et al. A Novel Method for Correcting Pelvic Tilt on Anteroposterior Pelvic Radiographs. Cureus. 2019;11(12):e6274.
19. Siebenrock KA, Kalbermatten DF, Ganz R. Effect of pelvic tilt on acetabular retroversion: a study of pelves from cadavers. Clin Orthop Relat Res. 2003(407):241-8.

20. Tatka J, Delagrammaticas D, Kemler BR, Rosenberg SI, Brady AW, Bryniarski AR, et al. A new understanding of radiographic landmarks of the greater trochanter that indicate correct femoral rotation for measurement of femoral offset. Arthroplasty. 2022;4(1):21.
21. Kanazawa M, Nakashima Y, Arai T, Ushijima T, Hirata M, Hara D, et al. Quantification of pelvic tilt and rotation by width/height ratio of obturator foramina on anteroposterior radiographs. Hip Int. 2016;26(5):462-7.
22. Hofman A, Jaddoe VW, Mackenbach JP, Moll HA, Snijders RF, Steegers EA, et al. Growth, development and health from early fetal life until young adulthood: the Generation R Study. Paediatr Perinat Epidemiol. 2004;18(1):61-72.
23. Kooijman MN, Kruithof CJ, van Duijn CM, Duijts L, Franco OH, van Ijzendoorn MH, et al. The Generation R Study: design and cohort update 2017. European Journal of Epidemiology. 2016;31(12):1243-64.
24. Smith-Bindman R, Chu PW, Azman Firdaus H, Stewart C, Malekhedayat M, Alber S, et al. Projected Lifetime Cancer Risks From Current Computed Tomography Imaging. JAMA Intern Med. 2025;185(6):710-9.
25. Rathnayaka K, Momot KI, Noser H, Volp A, Schuetz MA, Sahama T, et al. Quantification of the accuracy of MRI generated 3D models of long bones compared to CT generated 3D models. Med Eng Phys. 2012;34(3):357-63.
26. Van den Broeck J, Vereecke E, Wirix-Speetjens R, Vander Sloten J. Segmentation accuracy of long bones. Med Eng Phys. 2014;36(7):949-53.
27. Kamphuis MA, Oei EHG, Runhaar J, Hanff D, Bierma-Zeinstra SMA, Klein S, et al. ENHANCING MODEL PERFORMANCE IN HIP JOINT SEGMENTATION BY LEVERAGING MULTIPLE IMAGE OUTPUTS FROM DIXON MRI. Osteoarthritis Imaging. 2024;4:100193.
28. Kamphuis MA, Oei EHG, Runhaar J, Hanff DF, Tolk JJ, Agricola R, et al. EXPLORING SEX-BASED HIP MORPHOLOGY DIFFERENCES IN YOUNG ADULTS USING AN AUTOMATED 3D METHOD. Osteoarthritis Imaging. 2025;5:100295.
29. Greenway K, Knipe H, Gaillard F. Hounsfield unit. Reference article, Radiopaedia.org [Accessed on: 15 Feb 2026].
30. Gopalakrishnan V, Golland P, editors. Fast auto-differentiable digitally reconstructed radiographs for solving inverse problems in intraoperative imaging. Workshop on Clinical Image-Based Procedures; 2022: Springer.
31. Lindner C, Thiagarajah S, Wilkinson JM, arcOGEN Consortium, Wallis GA, Cootes TF. Fully automatic segmentation of the proximal femur using random forest regression voting. IEEE Trans Med Imaging. 2013;32(8):1462-72.
32. Akaike H. A new look at the statistical model identification. IEEE Transactions on Automatic Control. 1974;19(6):716-23.
33. Van Rossum G, Drake FL. Python reference manual: Centrum voor Wiskunde en Informatica Amsterdam; 1995.
34. Virtanen P, Gommers R, Oliphant TE, Haberland M, Reddy T, Cournapeau D, et al. SciPy 1.0: fundamental algorithms for scientific computing in Python. Nature Methods. 2020;17(3):261-72.

Appendix A

Overview of BoneFinder landmarks in the obturator foramen

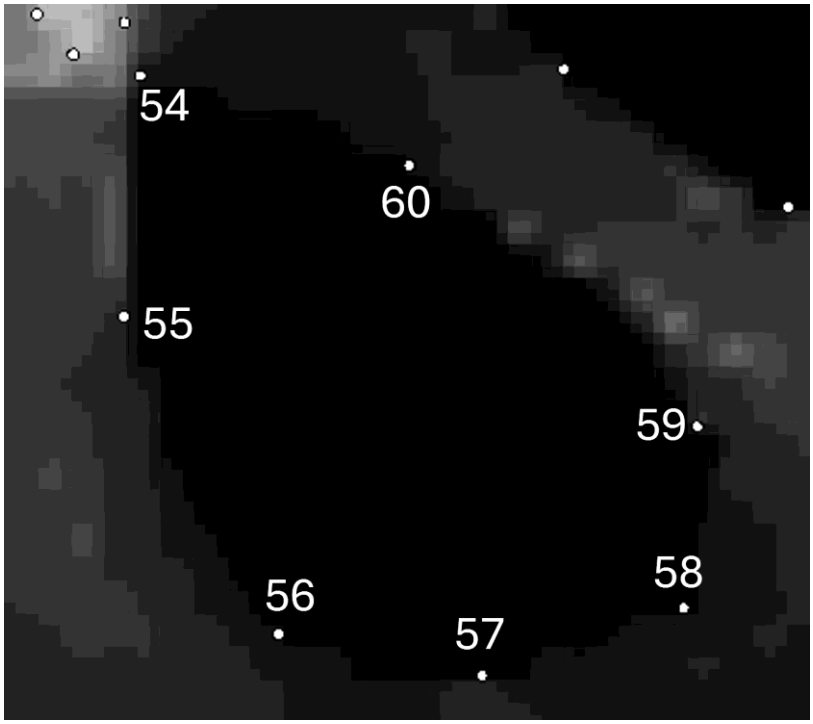

Point (54): In the superolateral corner of the obturator foramen.
Point (55): Equally spaced between (54) and (56), following the contour of the lateral rim of the obturator foramen.
Point (56): In the inferolateral corner of the obturator foramen.
Point (57): Place this point equally spaced between (56) and (58), following the contour/angle of the inferior rim of the obturator foramen.
Point (58): In the inferomedial corner of the obturator foramen.
Point (59): In the superomedial corner of the obturator foramen.
Point (60): Place this point equally spaced between (59) and (54), following the contour/angle of the superior rim of the obturator foramen

Boel F, Riedstra NS, Tang J, Hanff DF, Ahedi H, Arbabi V, et al. Reliability and agreement of manual and automated morphological radiographic hip measurements. Osteoarthr Cartil Open. 2024;6(3):100510.